Mapping piezoelectric response in nanomaterials using a dedicated non-destructive scanning probe technique

Yonatan Calahorra[1], Michael Smith[1], Anuja Datta[1], Hadas Benisty[2], Sohini Kar-Narayan[1]*

[1] *Department of Materials Science and Metallurgy, University of Cambridge, 27 Charles Babbage Road, Cambridge CB3 0FS, UK*

[2] *Department of Electrical Engineering, Technion-ITT, Haifa 32000, Israel*

email: sk568@cam.ac.uk

Supporting Information

ND-PFM operation:

The operation of ND-PFM often requires the imaging the area of interest by a non-destructive method (tapping), withdrawing the cantilever, and re-engaging to the same location. In the extreme case of the flat calibration sample, the results of which are discussed in the main text, the location of the domain boundary needs to be spatially identified, since there is no obvious geometrical indication that the high-speed data is indeed acquired across the boundary. Figure S1a shows a series of images obtained by peak-force QNM (left) and c-PFM (centre, right), where the contact mode images show that indeed the scanned area is across two opposite domains (right), and a distinct feature (dashed red circle) was identified. That feature was later found in the peak-force mode (dashed red circle, left image) used to obtain high-speed deflection data across the domain boundary. Figure S1b shows a schematic representation of the peak-force mode, on top of which the ND-PFM is implemented (as schematically shown in the main text).

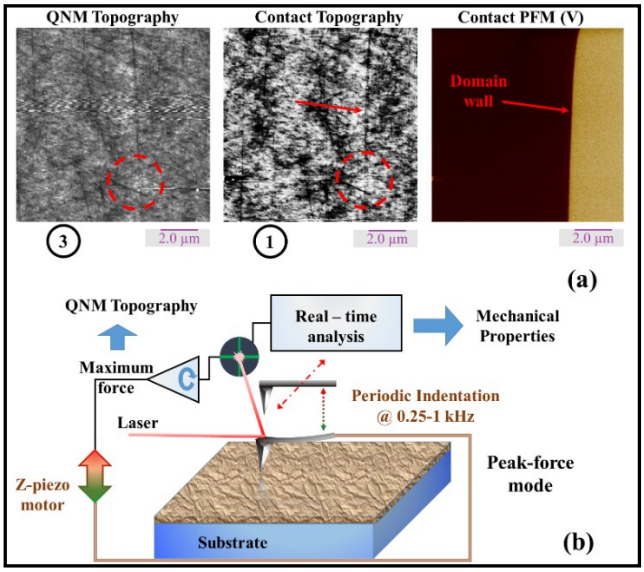

Figure S1. a) validation of tip position while switching from c-PFM to ND-PFM; b) Schematics of peak-force operation and signals. This mode is the basis for ND-PFM operation, and schematic is the basis for the one found in the main text. Numbers 1 & 3 correspond to Figure 1 in the main text.

Figure S2 describes the ND-PFM signal acquisition and analysis process, based on measurements of a ~300 nm PLLA NW, lying parallel to the cantilever; the results are discussed in detail in the main text. It starts by peak-force scanning the region of interest as shown in Figure S2a. The maximum length of a high-speed data capture instance in the *Multimode VIII* AFM is slightly over two seconds; therefore, by setting the scan rate and scan size such that a single line is completed in two seconds, the high-speed scans can be made to correlate with the peak-force imaging.

There are two "very" high speed channels, taken at f_{HSDC} = 6.25 MHz, set to collect vertical and lateral deflection data, and two "moderate" high speed channels, at 50 kHz, usually set to record height data (as shown in Figure S2b – this is not a cross section from the topography image) and the force error (the signal which is fed back for control). Figures S2c,d show the raw vertical deflection data (complete and zoomed-in); the deflection peaks correspond to tip/sample contact, and to the 'times of interest' in terms of PFM analysis. Note the gap in deflection data corresponding to when the tip slides down the NW to the surface; we ignore the data obtained there as the nature of the tip/sample interaction is not clear, and it seems the tip is moved before reaching a significant deflection.

The ratio of high speed and PFM frequencies dictates the number of high speed samples constructing a complete PFM period

$$N_{smpl,min} = \frac{f_{HSDC}}{f_{PFM}} = \frac{6250}{125} = 50 \quad (1)$$

We use an integer multiplication of this number, typically N_{smpl} = 2000 – 4000 samples spanning 40 – 80 periods of the PFM signal; such a batch of samples will yield a *single data point, per single deflection curve*. Each sample set is then fitted to a 2nd degree polynomial, and the result is further subtracted from the data (Figure S2e), emulating a low-pass filter operation, as done in lock-in amplifiers. Next, each of the "cleaned" data sets, X_{data}, is fed to the virtual lock-in (see code in data repository for implementation)

$$Cor(t) = \cos\left(2\pi f_{pfm} \cdot t + \varphi\right) + j \cdot \sin\left(2\pi f_{pfm} \cdot t + \varphi\right) \quad (2)$$

$$Inphase = Real\left\{\frac{1}{T}\int Cor(t) \cdot X_{data}(t)dt\right\}$$

$$Quadrature = Img\left\{\frac{1}{T}\int Cor(t) \cdot X_{data}(t)dt\right\}$$

the result is then an in-phase and quadrature (out-of-phase) value, or amplitude and phase, of the signal in f_{PFM}.

Following Jungk et al.[1], in order to nullify the quadrature signal, the phase, φ, is arbitrarily changed such that the standard deviation of that channel is minimized, leaving the physically relevant

data in the inphase channel. Note that this does not eliminate background noise. Figure S2f,g show different inphase and quadrature signals obtained from the raw data presented in Figure S2c, where Figure S2f shows the minimized quadrature, and the zoom in to relevant scale shows the different PFM signals obtained for the NW and the substrate. The large negative peak in the inphase channel is ignored as it stems from time periods where tip-NW contacts was not well established (Figure S2c).

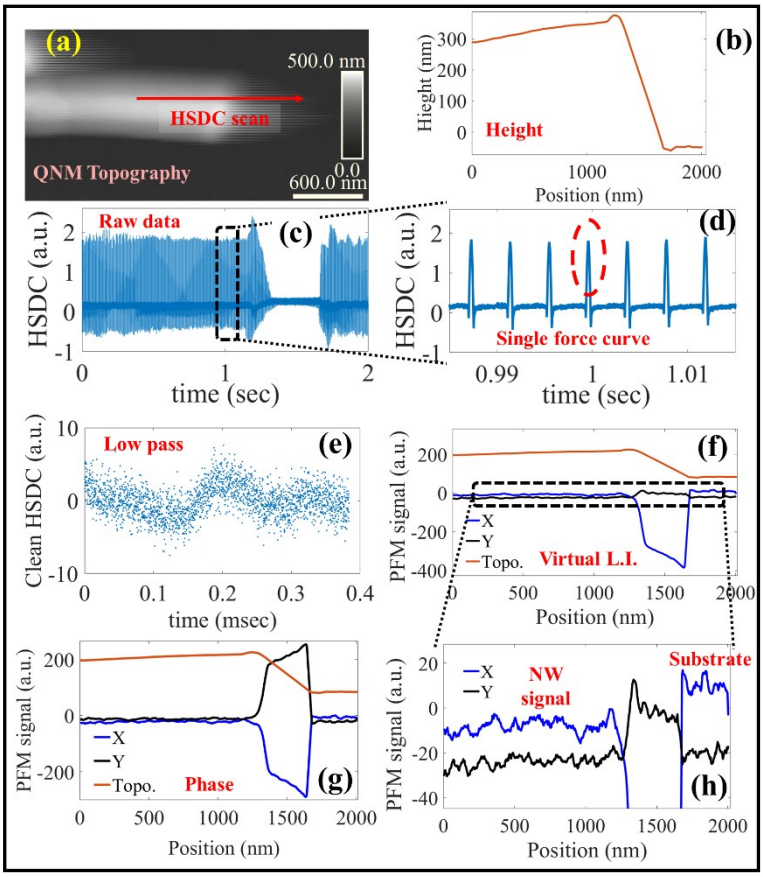

Figure S2. Representative signals obtained during ND-PFM of PLLA NWs: a) A preliminary peak-force scan; b) The HSDC recorded height; c) Raw vertical deflection data; d) Close-up of the raw vertical deflection data in [c]; e) Single force-curve data after removing low frequency components; f) Virtual lock-in output overlaid on topography; g) Same as [f] with different lock-in phase; h) Close-up view of [f] showing the NW and substrate signals. The signals obtained from the deflection gap in [c] correspond to the tip coming down form the NW to the substrate and are disregarded.

Signals in ND-PFM:

Figure S3 shows a series of images illustrating the averaging of the inphase signal in the regular operation of peak-force mode, when superimposing PFM operation on that mode by applying a voltage and observing lock-in amplifier output. Figure S3a shows the PFM inphase signal obtained from a horizontal GaAs NW of about 90 nm; a cross-section of that image is shown in Figure S3b, showing the different values obtained from the NW, and the conductive substrate on which it was dispersed. Figures S3c,d show the PFM inphase signals obtained while indenting the NW and substrate, respectively, as marked by the (c) and (d) points. The inphase signal and deflection are presented simultaneously, clearly demonstrating the significant change in signal when the tip is/not in contact with the sample. Figures S3e,f show a close-up to the PFM signal during contact, indicating the "real" values obtained from the sample, which are distinct (NW and surface), and both very different from the averaged value presented by the AFM software. These are the values which are targeted by ND-PFM, the averaged values are dominated by non-contact signals.

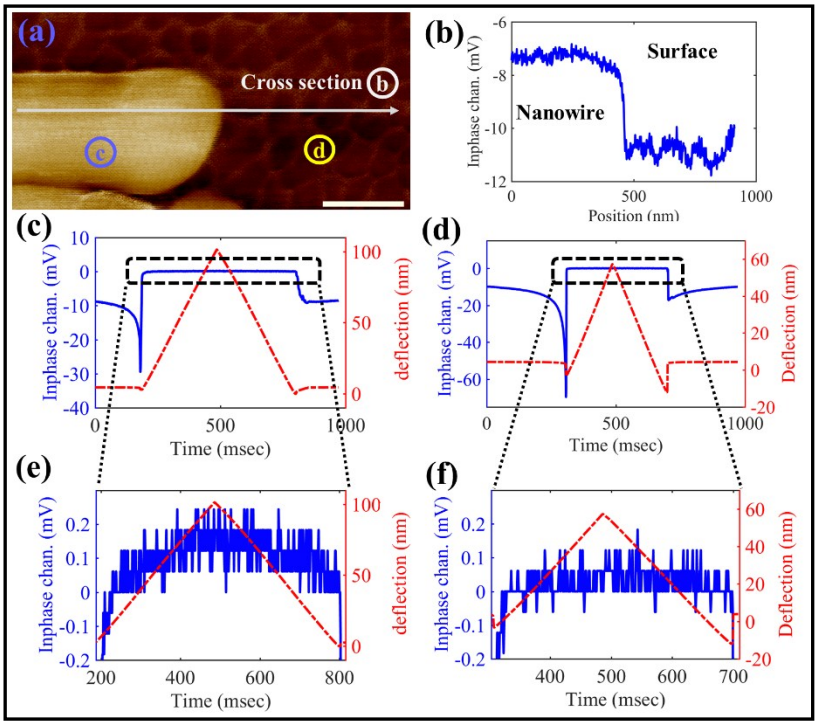

Figure S3. Averaging of PFM signals in peak-force mode: a) Inphase channel output scanned during peak-force mode scan of a horizontal GaAs NW on gold; b) Inphase channel cross-section; c) Inphase channel output during local nanoindentation (similar to single peak-force indentation cycle) obtained from the NW; d) Inphase channel output during local nanoindentation of the surface; e) close-up to [c]; f) close-up to [d].

In order to extract quantitative results, two calibration operations were performed. Firstly, the PPLN calibration sample was measured, and using the 7.5 pm/V d_{33} value indicated by *Bruker* the calibration yielded ~0.5 pm/a.u. for the vertical signal, and ~0.1 pm/a.u. for the lateral signal, following the derivation by Peter *et al.*[2], and the cantilever's dimensions measured previously[3].

However, due to the reported large contact potential difference found on the PPLN sample by Kim *et al.[4]* (a result we have successfully reproduced – data not shown) which may induce large electrostatic contributions to the calibration signal, we have performed a second calibration procedure based on a 100 nm poly (vinylidene fluoride-trifluoroethylene) (PVDF-TrFE) film, where a minimal d_{33} coefficient of 10 pm/V [5] was used. Figure S4 shows the c-PFM and ND-PFM of the poled region. The difference between the values obtained for the poled and unpoled regions in a.u. for a 6V AC amplitude the value of ~ 0.4 pm/a.u. is obtained for the vertical signal leading to a similar ~ 0.1pm/a.u. value for the lateral signals.

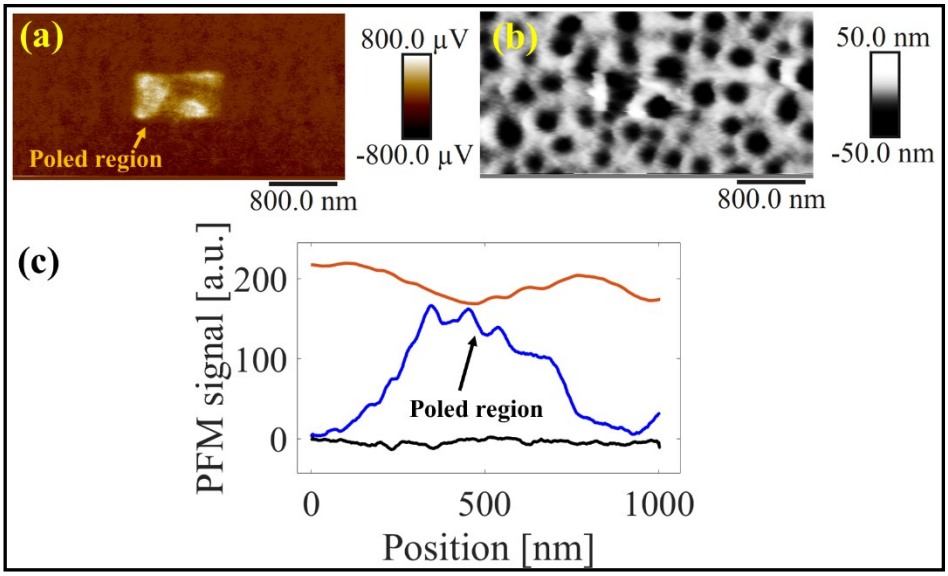

Figure S4. Poling of a 100 nm PVDF-TrFE film used for calibration: a) vertical c-PFM signal showing the polarized region; b) topography of the area shown in [a]; c) ND-PFM measurements of the same region clearly showing the signal arising from poled region (~ 150 a.u.) and the unpoled regions (~ 0 a.u.).

The BCT-BZT NW mesh measurements were conducted using a different tip, which resulted in 0.3 pm/a.u. and ~ 0.07 pm/a.u. for the vertical and lateral sensitivity, correspondingly. The PLLA NWs were measured by a tip which was not calibrated however similar values are expected considering the tip is the same model as all those reported here and the high consistency of the calibration values.

Nonetheless, we should note that the lateral sensitivity is only assessed following a literature based calculation and not measured directly for these tips. A challenge which needs to be further addressed in order to retrieve trustworthy quantitative results.

BCT-BZT NW network ND-PFM:

As mentioned in the main text, performing c-PFM in this sample proved unsuccessful. Figure S5a shows the results obtained while attempting c-PFM. On the left hand side, the tapping mode topography of the NW network is clearly shown, however the contact mode topography and PFM images clearly show no usable data. In our previous publication this has led us to focus on a single point PFM spectroscopy, rather than mapping piezoresponse. Figure S5b shows the consistency of the obtained signal in two separate scans, and Figure S5c the results obtained from a different location with similar characteristic values.

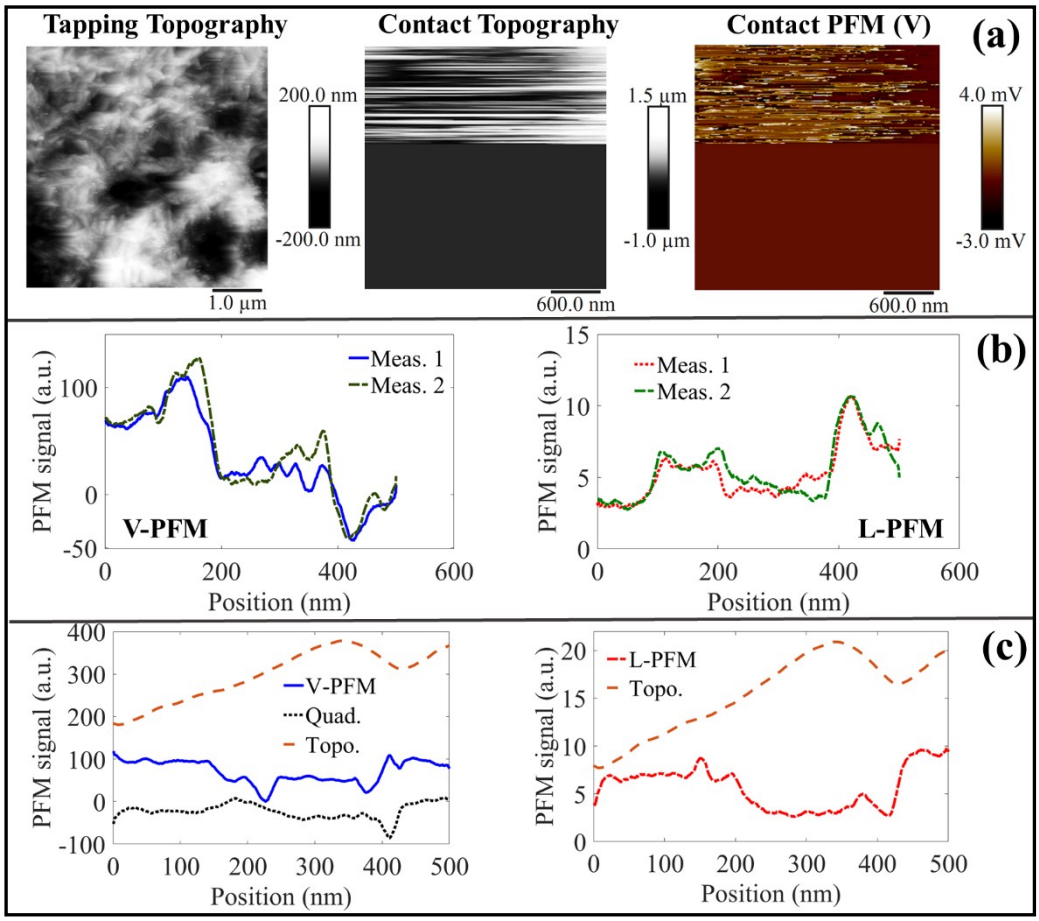

Figure S5. ND-PFM of BCT-BZT NW network. a) Tapping mode (left) and contact mode topography (middle) and V-PFM (right), demonstrating the inability of using c-PFM on this material; b) two scans obtained from the same location; c) a scan obtained from a different location.

References

1. Jungk, T., A. Hoffmann, and E. Soergel, *Consequences of the background in piezoresponse force microscopy on the imaging of ferroelectric domain structures.* Journal of Microscopy-Oxford, 2007. **227**(1): p. 72-78.
2. Peter, F., et al., *Comparison of in-plane and out-of-plane optical amplification in AFM measurements.* Review of Scientific Instruments, 2005. **76**(4).
3. Smith, M., et al., *Direct observation of shear piezoelectricity in poly-l-lactic acid nanowires*. 2017, AIP: APL Materials. p. 074105.
4. Kim, S., et al., *Electrostatic-free piezoresponse force microscopy.* Scientific Reports, 2017. **7**.
5. Calahorra, Y., et al., *Localized electromechanical interactions in ferroelectric P(VDF-TrFE) nanowires investigated by scanning probe microscopy.* Apl Materials, 2016. **4**(11): p. 9.
6. Datta, A., et al., *Lead-Free Polycrystalline Ferroelectric Nanowires with Enhanced Curie Temperature.* Advanced Functional Materials, 2017: p. 1701169.